

# Synthesis, metalation and antiaromatic properties of 22-hydroxybenziporphyrins

# Timothy D. Lash<sup>⋄</sup>\*, Sun T. Chaney, Amy L. Johnson, Jack T. Weisbond and Gregory M. Ferrence

Department of Chemistry, Illinois State University, Normal, Illinois 61790-4160, USA

Received 16 June 2021 Accepted 20 July 2021

Dedicated to Professors Lechosław Latos-Grażyński and Hiroyuki Furuta on the occasion of their 70th and 65th birthdays, respectively

**ABSTRACT:** Condensation of 5-alkyl-2-hydroxybenzene-1,3-dicarbaldehydes with a tripyrrane in the presence of trifluoroacetic acid (TFA), followed by oxidation with 2,3-dichloro-5,6-dicyano-1,4-benzoquinone (DDQ), gave two examples of 22-hydroxybenziporphyrins. Unlike a related *meso*-tetraphenyl-22-hydroxybenziporphyrin, these products were reasonably stable in solution. Dicationic species were obtained upon addition of TFA to CDCl<sub>3</sub> solutions, and these exhibited weakly diatropic properties. However, the free base forms gave broad peaks for the macrocycle's peripheral protons that fell into the range of 4.5–3.3 ppm, demonstrating that the system has paratropic characteristics that are consistent with the keto-tautomers. The porphyrin analogues gave broad, poorly resolved, UV-vis spectra of the type expected for nonaromatic or antiaromatic structures. Reaction of a hydroxybenziporphyrin with nickel(II), copper(II) or palladium(II) acetate gave the related coordination complexes. The nickel and palladium derivatives were structurally characterized by X-ray crystallography and exhibited buckled geometries with the phenolate units strongly pivoted away from the macrocyclic core.

**KEYWORDS:** benziporphyrins, carbaporphyrinoids, antiaromaticity, "3 + 1" MacDonald synthesis.

# INTRODUCTION

Immediately following the discovery of N-confused porphyrins 1 by Furuta and Latos-Grażyński in 1994 [1–4], a number of structurally similar carbaporphyrinoid systems [5] were reported including benziporphyrins 2 [6], carbaporphyrins (e.g. 3) [7], azuliporphyrins 4 [8] and tropiporphyrins 5 [9] (Fig. 1). In our earliest contribution to this field [10], we speculated that 2-hydroxybenziporphyrin 6 could tautomerize to give an aromatic porphyrinoid named oxybenziporphyrin (7). Condensation of 4-hydroxyisophthalaldehyde with tripyrrane 8 in the presence of trifluoroacetic acid (TFA), followed by oxidation with 2,3-dichloro-5,6-dicyano-1,4-benzoquinone (DDQ),

Correspondence to: Timothy D. Lash, email: tdlash@ilstu.edu.

afforded dark green solutions of an aromatic porphyrinoid that proved to be the anticipated semiquinone species 7 (Scheme 1) [10]. The same strategy was applied to the synthesis of oxypyriporphyrin [11, 12]. In essence, hydroxybenziporphyrin 6 undergoes a keto-enol-like tautomerization to give a fully aromatic form, and the comparative favorability for the keto-tautomer was later confirmed with DFT calculations [13]. Oxybenziporphyrins can act as trianionic ligands, giving stable silver(III) [14] and gold(III) [15] organometallic derivatives. However, 7 can also potentially act as a dianionic ligand generating palladium(II) and platinum(II) complexes [16, 17].

Following the successful synthesis of oxybenziporphyrin [10], structural variants of this system were investigated [18]. In one study [19], 2-hydroxy-5-methyl-1,3-benzenedicarbaldehyde (9) was condensed with tripyrrane 8 in the presence of TFA in an attempt to introduce

SPP full member in good standing.

Fig. 1. Structures of selected carbaporphyrinoids.

a hydroxyl substituent at the 22-position (Scheme 2). It was speculated that oxidation of the initially formed 22-hydroxybenziporphyrin 10 might afford an aromatic keto-derivative 11 [19]. Porphyrinoid 10 was isolated in 23% yield but all attempts to oxidize this product to 11 were unsuccessful. In retrospect, this conversion was not

Scheme 1. Synthesis of oxybenziporphyrin.

Scheme 2. Synthesis of 22-hydroxybenziporphyrin.

likely to be successful given the presence of so many lone pair electrons within the macrocyclic cavity. Preliminary coordination studies on 10 were also conducted [20] but until this point no details on these investigations have been published.

Although initial explorations of benziporphyrins were conducted on meso-unsubstituted structures, a route to meso-tetraarylbenziporphyrins 12 was subsequently reported by Stepien and Latos-Gražynski [21, 22] and later modified by others [23]. In addition to exploring the coordination chemistry of benziporphyrins [21-25], Stepien and Latos-Gražynski showed that tetraphenylbenziporphyrin was oxidized with silver(I) acetate to give 22-acetoxybenziporphyrin 13 (Scheme 3) [21] and the same chemistry was later used to prepare 22-acetoxy-2,4-dimethoxybenziporphyrins [26]. Acidcatalyzed hydrolysis afforded the bis-hydrochloride salt of 22-hydroxybenziporphyrin 14, and the proton NMR spectrum for this species indicated that the macrocycle possessed weakly diatropic characteristics. In addition, a series of Zn, Cd, Ni(II), Pd(II) and Fe(III) complexes 15 of hydroxybenziporphyrin were prepared from 14 or directly from 13 [27]. Careful neutralization of solutions containing 14 with sodium hydroxide gave the related 22-hydroxybenziporphyrin 16 [28]. However, unlike 9, 16 proved to be very unstable. At 303 K, the proton NMR spectrum of 16 in CD<sub>2</sub>Cl<sub>2</sub> gave broad poorly resolved peaks that were attributed to a temperature dependent dynamic process. Following deuterium exchange, the proton NMR spectrum of 16 at 193 K gave rise to two sets of proton resonances that were consistent with the presence of two different species, an antiaromatic keto-form 17 in addition to the hydroxy-tautomer 16. Keto-tautomer 17 possesses a  $20\pi$  electron circuit, highlighted in bold, that gives

Scheme 3. Tetraphenyl 22-hydroxybenziporphyrin.

rise to the observed paratropic ring current. Intriguingly, DFT calculations showed that antiaromatic tautomer **17** is 3.35 kcal/mol more stable than **16** [28]. Furthermore, for unsubstituted 22-hydroxybenziporphyrin, the ketotautomer was calculated to be 8.34 kcal/mol more stable than the phenolic form.

In this paper, syntheses of *meso*-unsubstituted 22-hydroxybenziporphyrins are reported and the results are contrasted to the *meso*-substituted series. In addition, nickel(II), copper(II) and palladium(II) complexes have been prepared, two of which have been structurally characterized by X-ray crystallography.

#### **EXPERIMENTAL**

Melting points are uncorrected. NMR spectra were recorded on a 500 MHz NMR spectrometer and were run at 302 K unless otherwise indicated.  $^{1}$ H NMR values are reported as chemical shifts  $\delta$ , relative integral, multiplicity (s, singlet; d, doublet; t, triplet; q, quartet; m, multiplet; br, broad peak) and coupling constant (J). Chemical shifts are reported in parts per million (ppm) relative to CDCl<sub>3</sub> ( $^{1}$ H residual CHCl<sub>3</sub>  $\delta$  7.26,  $^{13}$ C CDCl<sub>3</sub> triplet  $\delta$  77.23) or CD<sub>2</sub>Cl<sub>2</sub> (1H residual CHDCl<sub>2</sub>  $\delta$  5.32,

<sup>13</sup>C CDCl<sub>3</sub> pentet δ 53.1) and coupling constants were taken directly from the spectra. NMR assignments were made with the aid of <sup>1</sup>H–<sup>1</sup>H COSY, HSQC, DEPT-135 and nOe difference proton NMR spectroscopy. 2D experiments were performed by using standard software. <sup>1</sup>H and <sup>13</sup>C NMR spectra for all new compounds are reported in the supplementary materials.

22-Hydroxy-9,13,14,18-tetraethyl-3,8,19-trimethylbenziporphyrin (10a). Tripyrrane dicarboxylic acid 9 (100 mg, 0.22 mmol) was stirred with TFA (5 mL) for 2 min under nitrogen, Dichloromethane (180 mL) was added, followed immediately by 2-hydroxy-5-methyl-1,3 benzenedicarbaldehyde (36.2 mg. 0.22 mmol) and the mixture was stirred in the dark under nitrogen for 4 h. The solution was neutralized by the dropwise addition of triethylamine, DDO (51 mg) was added, and the mixture stirred for 30 min. The solution was washed with water, the solvent was removed on a rotary evaporator, and the residue purified on a grade 3 alumina column, eluting with chloroform. A reddish fraction was collected, the solvent evaporated under reduced pressure and the residue triturated with hexanes and suction filtered to give the benziporphyrin (59.5 mg, 0.121 mmol, 55%) a dark green solid, mp >260 °C. UV-vis (CH<sub>2</sub>Cl<sub>2</sub>):  $\lambda_{max}$ / nm  $(\log \varepsilon)$  284 (4.25), 331 (4.26), 447 (4.38), 584 (sh, 3.50). UV-vis (100 equiv. TFA-CH<sub>2</sub>Cl<sub>2</sub>):  $\lambda_{max}/nm$  (log  $\epsilon$ ) 287 (4.40), 330 (sh, 4.44), 352 (sh, 4.57), 364 (4.62), 448 (4.73). UV-vis (1% TFA-CH<sub>2</sub>Cl<sub>2</sub>):  $\lambda_{max}/nm$  (log  $\epsilon$ ) 289 (4.28), 322 (sh, 4.37), 365 (4.60), 444 (4.58), 506 (sh, 3.93). UV-vis (10% TFA-CH<sub>2</sub>Cl<sub>2</sub>):  $\lambda_{max}/nm$  (log  $\epsilon$ ) 312 (4.50), 366 (4.63), 404 (4.57), 501 (sh, 4.00), 571 (sh, 3.43), 751 (3.45). UV-vis (1% DBU-CH<sub>2</sub>Cl<sub>2</sub>):  $\lambda_{max}$ nm (log ε) 372 (4.47), 586 (4.01). <sup>1</sup>H NMR (500 MHz, TFA-CDCl<sub>3</sub>): δ 7.56 (s, 2H, 2,4-H), 7.50 (s, 2H, 6,21-H), 6.76 (s, 2H, 11,16-H), 2.86 (q, 4H, J = 7.7 Hz), 2.82  $(q, 4H, J = 7.7 Hz) (4 \times CH_2CH_3), 2.53 (s, 6H, 8,19 CH_3$ ), 2.34 (s, 3H, 3- $CH_3$ ), 1.34 (t, 6H, J = 7.7 Hz), 1.29 (t, 6H, J = 7.7 Hz) (4 × CH<sub>2</sub>CH<sub>3</sub>). <sup>1</sup>H NMR (500 MHz,  $CD_2Cl_2$ , 233 K):  $\delta$  4.28 (s, 2H), 3.35 (s, 2H), 3.28 (s, 2H), 1.55 (q, 4H, J = 7.6 Hz), 1.50 (q, 4H, J = 7.6 Hz), 1.16 (s, 6H), 0.95 (s, 3H), 0.68-0.62 (m, 12H). <sup>13</sup>C{H} NMR (125 MHz, TFA-CDCl<sub>3</sub>): δ 156.8, 154.2, 146.8, 146.2, 142.5. 141.7 (2,4-CH), 140.5, 138.6, 127.8 (6,21-CH), 125.6, 94.2 (11,16-CH), 20.0 (3-CH<sub>3</sub>), 18.3, 18.0  $(4 \times CH_2CH_3)$ , 15.1, 14.4  $(4 \times CH_2CH_3)$ , 10.3 (8,19-CH<sub>3</sub>).  ${}^{13}$ C{H} NMR (125 MHz, CD<sub>2</sub>Cl<sub>2</sub>):  $\delta$  172.2, 156.3, 145.5 (2,4-CH), 145.0, 143.4, 137.1, 136.9, 131.7, 131.3, 125.2 (6,21-CH), 96.0 (11,16-CH), 17.2 (3-Me), 16.3, 15.8 ( $4 \times CH_2CH_3$ ), 14.0, 12.7 ( $4 \times CH_2CH_3$ ), 7.5 (8,19-CH<sub>3</sub>). HR-MS (ESI) m/z: [M + H]<sup>+</sup> calcd for C<sub>33</sub>H<sub>38</sub>N<sub>3</sub>O 492.3015, found 492.2996. HR-MS (EI) m/z: [M + 2H]<sup>+</sup> calcd for C<sub>33</sub>H<sub>39</sub>N<sub>3</sub>O 493.3093, found 493.3087.

3-tert-Butyl-22-Hydroxy-9,13,14,18-tetraethyl-8,19-dimethylbenziporphyrin (10b). Tripyrrane 9 (100 mg, 0.22 mmol) was reacted with 4-tert-butyl-2-hydroxy-benzene-1,3-dicarbaldehyde (45.5 mg, 0.22 mmol) under the foregoing conditions to give the title compound

(43.2 mg, 0.081 mmol, 37%) as a dark green solid, mp >260 °C. UV-vis (CH<sub>2</sub>Cl<sub>2</sub>):  $\lambda_{max}/nm$  (log  $\epsilon$ ) 286 (4.32), 330 (4.51), 370 (sh, 4.33), 448 (4.65), 580 (sh, 3.82). UV-vis (20 equiv. TFA-CH<sub>2</sub>Cl<sub>2</sub>):  $\lambda_{max}$ /nm (log  $\epsilon$ ) 289 (4.39), 330 (sh, 4.52), 352 (sh, 4.65), 365 (4.71), 448 (4.81). UV-vis (1% TFA-CH<sub>2</sub>Cl<sub>2</sub>):  $\lambda_{max}/nm$  (log  $\epsilon$ ) 289 (4.35), 330 (sh, 4.47), 351 (sh, 4.60), 365 (4.67), 448 (4.77). UV-vis (10% TFA-CH<sub>2</sub>Cl<sub>2</sub>):  $\lambda_{max}/nm$  (log  $\epsilon$ ) 313 (4.56), 367 (4.68), 406 (4.63), 500 (sh, 4.06), 572 (sh, 3.50), 759 (3.52). UV-vis (1% DBU-CH<sub>2</sub>Cl<sub>2</sub>):  $\lambda_{max}/nm$  $(\log \varepsilon)$  371 (4.54), 582 (sh, 3.99). 621 (4.01), 718 (sh, 3.48). <sup>1</sup>H NMR (500 MHz, TFA-CDCl<sub>3</sub>): δ 7.50 (s, 2H, 2,4-H), 7.25 (s, 2H, 6,21-H), 6.46 (s, 2H, 11,16-H), 2.77-2.70 (m,  $4 \times CH_2CH_3$ ), 2.45 (s, 6H,  $8,19-CH_3$ ), 1.30(t, 6H, J = 7.7 Hz), 1.32 (s, 9H, t-Bu), 1.25 (t, 6H, J =7.7 Hz)  $(4 \times CH_2CH_3)$ . <sup>1</sup>H NMR (500 MHz, CD<sub>2</sub>Cl<sub>2</sub>, 233 K): δ 4.50 (s, 2H), 3.49 (s, 2H), 3.35 (s, 2H), 1.74–1.70 (m, 4H), 1.59–1.52 (m, 4H), 1.20 (s, 6H), 0.69–0.61 (m, 21H). <sup>13</sup>C{H} NMR (125 MHz, TFA-CDCl<sub>3</sub>): δ 156.1, 154.1, 146.2, 145.0, 142.6, 140.1, 139.8 (2,4-CH), 129.0 (6,21-CH), 126.0, 94.2 (11,16-CH), 34.4 (C(CH<sub>3</sub>)<sub>3</sub>), 30.5  $(C(CH_3)_3)$ , 18.2, 17.9  $(4 \times CH_2CH_3)$ , 15.1, 14.4  $(4 \times CH_2CH_3)$  $CH_2CH_3$ ), 10.2 (8,19-CH<sub>3</sub>). <sup>13</sup>C{H} NMR (125 MHz,  $CD_2Cl_2$ ):  $\delta$  172.0, 156.5, 156.0, 145.0, 144.7, 145.5, 142.3 (2,4-CH), 137.1, 136.9, 136.9, 131.2, 125.4 (6,21-CH), 95.8 (11,16-CH), 31.4 ( $C(CH_3)_3$ ), 28.3 ( $C(CH_3)_3$ ), 16.4, 15.9 (4  $\times$  CH<sub>2</sub>CH<sub>3</sub>), 14.1, 12.8 (4  $\times$  CH<sub>2</sub>CH<sub>3</sub>), 7.6 (8,19-CH<sub>3</sub>). HR-MS (ESI) m/z: [M + H]<sup>+</sup> calcd for  $C_{36}H_{44}N_3O$  534.3484, found 534.3462.

*Nickel*(II) *complex* 19a. Nickel(II) acetate tetrahydrate (55 mg) in methanol (5 mL) was added to a solution of crude **10a** obtained by reacting **9** (100 mg, 0.22 mmol) and 8a (36.2 mg, 0.22 mmol) in chloroform (15 mL) and the mixture stirred at room temperature. The progress of the reaction was monitored by thin layer chromatography. When the reaction was complete (2-3 h), the mixture was washed with water, the solvent removed under reduced pressure, and the residue purified on grade 3 alumina eluting with dichloromethane and then chloroform. The product was collected as a yellow-orange fraction. Recrystallization from hexanes gave the nickel complex (45.4 mg, 0.0828 mmol, 37%) as dark purple crystals, mp >260 °C. UV-vis (CH<sub>2</sub>Cl<sub>2</sub>):  $\lambda_{max}/nm$  (log  $\epsilon$ ) 316 (4.49), 353 (4.61), 414 (4.45). <sup>1</sup>H NMR (500 MHz, CDCl<sub>3</sub>): δ 6.85 (s, 2H, 2,4-H), 6.35 (s, 2H, 6,21-H), 5.83 (s, 2H, 11,16-H), 2.48–2.32 (m, 8H,  $4 \times CH_2CH_3$ ), 2.09 (s, 6H,  $8,19-CH_3$ , 2.07 (s, 3H, 3-CH<sub>3</sub>), 1.13 (t, 6H, J = 7.6 Hz), 1.08 (t, 6H, J = 7.6 Hz) (4 × CH<sub>2</sub>CH<sub>3</sub>). <sup>13</sup>C{H} NMR (125) MHz, CDCl<sub>3</sub>): δ 161.4, 157.3, 153.2, 144.9, 143.7, 143.0, 137.6, 135.4 (2,4-CH), 130.4, 129.5, 124.6 (6,21-CH), 93.5 (11,16-CH), 20.6 (3-Me), 18.0, 17.9 ( $4 \times CH_2CH_3$ ), 15.8, 14.6 ( $4 \times CH_2CH_3$ ), 10.8 (8,19-CH<sub>3</sub>). HR-MS (ESI) m/z: [M + H]<sup>+</sup> calcd for C<sub>33</sub>H<sub>36</sub>N<sub>3</sub>NiO 548.2212, found 548.2201.

Copper(II) complex 19b. Copper(II) acetate hydrate (40 mg) in methanol (5 mL) was added to a solution of the crude product obtained by reacting 9 (100 mg,

0.22 mmol) and **8a** (36.2 mg, 0.22 mmol) in chloroform (15 mL) and the mixture stirred at room temperature for 5 min. The reaction was worked up as described for the nickel complex, and the metalated derivative eluted as an orange-red fraction. Recrystallization from hexanes gave the copper complex (41.6 mg, 0.0752 mmol, 34%) as dark purple crystals, mp >260 °C. UV-vis (CH<sub>2</sub>Cl<sub>2</sub>):  $\lambda_{\text{max}}/\text{nm}$  (log  $\epsilon$ ) 292 (sh, 4.47), 318 (4.51), 371 (4.69), 534 (4.02), 725 (3,36). HR-MS (ESI) m/z: M<sup>+</sup> calcd for C<sub>33</sub>H<sub>35</sub>CuN<sub>3</sub>O 552.2076, found 552.2074.

Palladium(II) complex 19c. Prepared by the previous procedure by reacting crude 10a derived from 9 (100 mg, 0.22 mmol) and **8a** (36.2 mg, 0.22 mmol) with palladium(II) acetate (40 mg) in chloroform (10 mL) and acetonitrile (10 mL) for ca. 2 h. The product eluted as a dark red fraction. Recrystallization from hexanes gave the palladium complex (46.8 mg, 0.0785 mmol, 35%) as a dark solid, mp >260 °C. UV-vis (CH<sub>2</sub>Cl<sub>2</sub>):  $\lambda_{max}/nm$  $(\log \varepsilon)$  280 (4.52), 318 (sh, 4.44), 363 (4.61), 411 (4.37), 556 (3.92), 586 (sh, 3.85). <sup>1</sup>H NMR (500 MHz, CDCl<sub>3</sub>): δ 6.80 (s, 2H, 2,4-H), 6.52 (s, 2H, 6,21-H), 6.06 (s, 2H, 11,16-H), 2.59–2.46 (m, 8H,  $4 \times CH_2CH_3$ ), 2.21 (s, 6H,  $8,19-CH_3$ , 2.06 (s, 3H,  $3-CH_3$ ), 1.20 (t, 6H, J = 7.6 Hz), 1.14 (t, 6H, J = 7.6 Hz) (4 × CH<sub>2</sub>CH<sub>3</sub>). <sup>13</sup>C{H} NMR (125 MHz, CDCl<sub>3</sub>): δ 159.3, 156.2, 151.4, 144.5, 142.8, 136.7, 135.4 (2,4-CH), 130.7, 127.0, 126.8 (6,21-CH), 94.1 (11,16-CH), 20.4 (3-Me), 18.2, 18.0 ( $4 \times CH_2CH_3$ ), 16.0, 14.8 ( $4 \times CH_2CH_3$ ), 10.6 ( $8,19-CH_3$ ). HR-MS (ESI) m/z: [M + H]<sup>+</sup> calcd for C<sub>33</sub>H<sub>36</sub>N<sub>3</sub>NiO 596.1893, found 596.1893.

#### RESULTS AND DISCUSSION

Hydroxybenziporphyrins 10 were prepared using the "3 + 1" variant of the MacDonald condensation [29] (Scheme 4). Reaction of 2-hydroxy-5-methyl-1,3benzenedicarbaldehyde (9a) with tripyrrane dicarboxylic acid 8 [30] in the presence of TFA, followed by an oxidation step, afforded hydroxybenziporphyrin 10a in up to 55% yield. Crystallization from dichloromethane-hexanes gave lower yields but trituration of the product fractions with hexanes, followed by suction filtration, gave superior yields of reasonably pure material. Similarly, 5-tert-butyl-2-hydroxy-1,3-benzenedicarbaldehyde (8b) reacted with tripyrrane 9 to give tert-butyl 22-hydroxybenziporphyrin in 37% yield. The free base benziporphyrins were only sparingly soluble and proton NMR spectra were commonly obtained for the related dications 10H<sub>2</sub><sup>2+</sup> in TFA-CDCl<sub>3</sub>. The proton NMR spectrum for **10a**H<sub>2</sub><sup>2+</sup> gave the rise to three 2H singlets at 7.56, 7.50 and 6.76 ppm (Fig. 2) for the peripheral benzene and *meso*-protons, values that are inconsistent with strongly aromatic macrocycles. However, as was the case for the analogous tetraphenyl hydroxybenziporphyrin dication 14, the shifts are sufficiently shifted downfield to imply the presence of a weakly diatropic ring current. The carbon-13 NMR

**Scheme 4.** Synthesis and metalation of *meso*-unsubstituted 22-hydroxybenziporphyrins.

spectrum confirmed the presence of a plane of symmetry and showed the *meso*-carbons at 94.2 (11,16-CH) and 127.8 ppm (6,21-CH). Similar results were obtained for *tert*-butyl benziporphyrin dication  $10bH_2^{2+}$ . The electron impact mass spectrum of 10a gave a molecular ion at m/z 493.3087 rather than the expected molecular ion value of m/z 491.2937 for  $C_{33}H_{37}N_3O$ . However, the formation of an  $[M+2H]^+$  ion was not unexpected as benziporphyrins commonly show abnormally large  $[M+1]^+$  and  $[M+2]^+$  peaks when analyzed by EIMS [12, 31]. Analysis of 10a by TOF ESI MS gave the expected  $[M+H]^+$  peak at m/z 492.2996 corresponding to  $C_{36}H_{44}N_3O^+$  at m/z 534.3462 by TOF ESI MS.

The UV-vis spectra for **10a** and **10b** gave broad absorptions that were consistent with nonaromatic

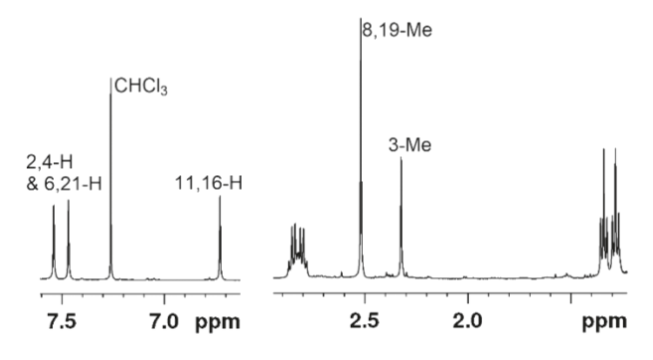
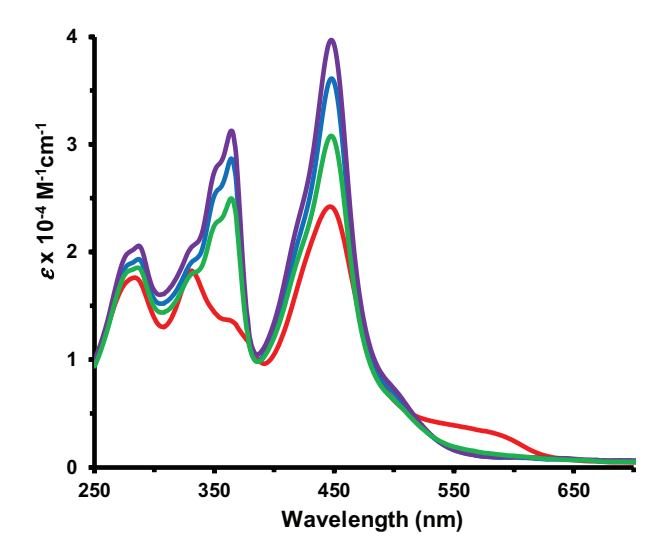


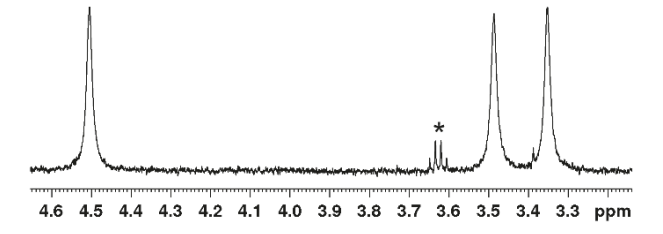
Fig. 2.500MHzprotonNMRspectrumofhydroxybenziporphyrin 10a in TFA-CDCl<sub>3</sub>.



**Fig. 3.** UV-vis spectra of 3-methyl 22-hydroxybenziporphyrin **10a** in CH<sub>2</sub>Cl<sub>2</sub> (red line) with 0 equiv (red), 0,5 equiv (green), 1 equiv (blue) and 2 equiv (purple) of TFA.

porphyrinoid structures. For instance, the UV-vis spectrum for 10b in CH<sub>2</sub>Cl<sub>2</sub> gave medium intensity absorptions at 284, 331 and 447 nm (Fig. 3). Electronic absorption spectra for free base porphyrin-type structures is often carried out in the presence of triethylamine to ensure that trace amounts of acid do not contaminate the solvent. However, for 10a and 10b, spectra run in 1% Et<sub>3</sub>N-CH<sub>2</sub>Cl<sub>2</sub> were significantly altered presumably due to partial deprotonation of the phenolic proton. In 1% DBU-CH<sub>2</sub>Cl<sub>2</sub>, **10a** and **10b** gave dark blue-green solutions but after 10 min significant decomposition took place. Addition of 2-3 equiv of TFA to solutions of 10 in CH<sub>2</sub>Cl<sub>2</sub> gave rise to a new species that was attributed to dication  $10H_2^{2+}$ . For 10b, this species gave peaks at 289, 365 and 448 nm (Fig. 3) and weaker absorptions at longer wavelengths. The spectra were only slightly modified 1% TFA-CH<sub>2</sub>Cl<sub>2</sub>, but further changes were observed in 10% TFA-CH<sub>2</sub>Cl<sub>2</sub>. Although the origin of the spectroscopic changes is not clear, it is worth noting that these processes are reversible. In addition, solutions of the protonated species derived from 10a and 10b were stable over a period of several hours.

In the initial investigations of **10a**, only poorly resolved NMR spectra could be obtained [19]. However, further investigation has revealed new insights into this system. Both **10a** and **10b** exhibit poor solubility characteristics but solutions in CD<sub>2</sub>Cl<sub>2</sub> showed the presence of broad absorptions between 3.3 and 4.5 ppm. These peaks were slightly more resolved at lower temperatures. At 233 K **10b** gave three 2H singlets for the *meso*- and external benzene protons at 4.50, 3.69 and 3.35 ppm (Fig. 4). Similarly, at this temperature **10a** afforded 2H singlets at 4.28, 3.35 and 3.33 ppm. The CH<sub>2</sub> resonances for the ethyl substituents could be identified between 1.5 and 1.8 ppm, while the pyrrole-CH<sub>3</sub> units appeared near



\* = solvent impurity

Fig. 4. Partial proton NMR spectrum of hydroxybenziporphyrin **10b** at 233 K in CD<sub>2</sub>Cl<sub>2</sub>.

1.2 ppm. The results show significant upfield shifts to the external protons that are consistent with the presence of a paratropic species and this suggestd that the system favors the antiaromatic keto tautomer "22-oxybenziporphyrin" 18 (Scheme 5). Importantly, the HSQC spectrum for 10a showed that the proton resonances at 4.28, 3.35 and 3.33 ppm corresponded to peaks at 96.0, 125.2 and 145.5 ppm in the carbon-13 NMR spectrum (Fig. 5), confirming that these signals result from sp<sup>2</sup> C-H units. The chemical shifts did not show significant changes with temperature, indicating that only one species is present at significant concentrations in solution. The results differ from those for tetraphenyl-22-hydroxybenziporphyrin where the phenol-tautomer is in equilibrium with the ketoform [28]. However, our results are consistent with the previously reported DFT calculations [28].

Metalation of 10a was also examined (Scheme 3). Reaction of 10a with nickel(II), copper(II) and palladium(II) acetate at room temperature afforded approximately 30% yield of the corresponding coordination complexes 19a-19c. Although 10a is fairly stable in solution, better overall results were obtained when the crude products from the reaction of 8 and 9a were directly metalated and this approach gave overall yields of 34–37% from 8 and 9a. Useful NMR data could not be obtained for

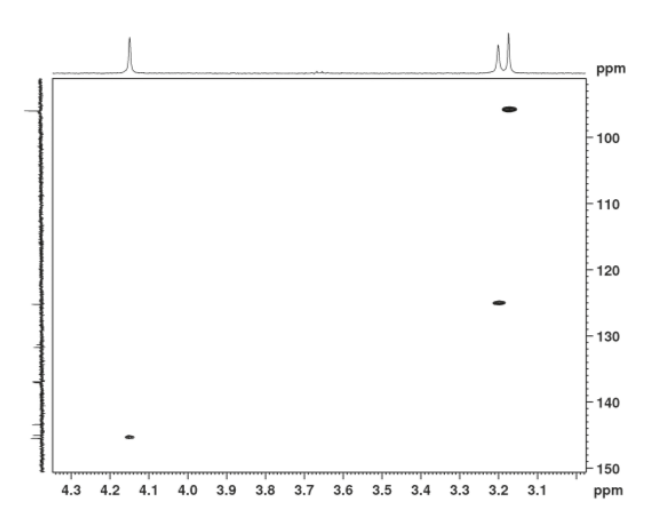


Fig. 5. HSQC spectrum of hydroxybenziporphyrin 10a in CD<sub>2</sub>Cl<sub>2</sub>.

**Scheme 5.** Conversion of 22-hydroxybenziporphyrins into antiaromatic 22-oxybenziporphyrins.

the paramagnetic copper(II) complex 19b, but nickel(II) and palladium(II) derivatives 19a and 19c gave good quality proton (Fig. 6) and carbon-13 NMR spectra. The results confirm that both of the structures retain a plane of symmetry and the macrocycles do not display diatropic characteristics. The meso-protons for 19a gave rise to two 2H singlets at 6.35 and 5.83 ppm, while the equivalent resonance for palladium complex 19c showed up at 6.52 and 6.06 ppm. In the carbon-13 NMR spectra, the *meso*-carbons at positions 11 and 16 gave resonances at 93.5 and 94.1 ppm, respectively, for 18a and 18c, while the carbons at positions 6 and 21 appeared at 124.6 and 126.8 ppm. The UV-vis spectra for **19a–19c** were again consistent with nonaromatic systems (Fig. 7). Nickel complex 19a gave medium-sized absorptions at 316, 352 and 414 nm, while copper complex 19b afforded peaks at 318, 371 and 534 nm. The UV-vis spectrum for palladium complex 19c was somewhat different, giving absorption bands at 280 348, 363, 411 and 556 nm (Fig. 7).

Crystals of 19a and 19c were identified that were suitable for X-ray diffraction analysis (Figs 8 and 9). These complexes are structurally similar to those reported for metalated oxyazuliporphyrins [32] and, to a lesser extent, coordination complexes of 21-hydroxy-N-confused porphyrins [33]. The molecular structure of nickel complex 19a (Fig. 8) shows that the porphyrinoid contains a metallotripyrrolic core which is slightly distorted from planarity. Relative to the mean plane defined by the conjugated tripyrrolic framework atoms, the pyrrole rings are tilted 1.33 (8) $^{\circ}$ , 5.79 (7) $^{\circ}$  and 8.66  $(9)^{\circ}$ , but the p-cresole moiety is canted by 28.55  $(3)^{\circ}$ . Bond distances and angles were generally validated using a Mogul geometry check [34]. While Mogul returned few hits for similar NiN<sub>3</sub>O bonding environments, the 1.9434 (12) Å, 1.8910 (12) Å and 1.9323 (12) Å Ni-N bond lengths are within the typical norms (1.93 (3) Å) for 4-coordinate nickel(II) containing porphyrinoid complexes. The 1.8335 (10) Å Ni-O distance is similarly within typical norms (1.86 (3)) for the NiN<sub>3</sub>O coordination environment. 19a exhibits a short 2.6814 (14) Å Ni1... C22 distance, which is significantly less than the sum of van der Waals radii (1.63 Å for Ni and 1.77 Å for C) [35]. Although a related tetraphenyl nickel(II) complex

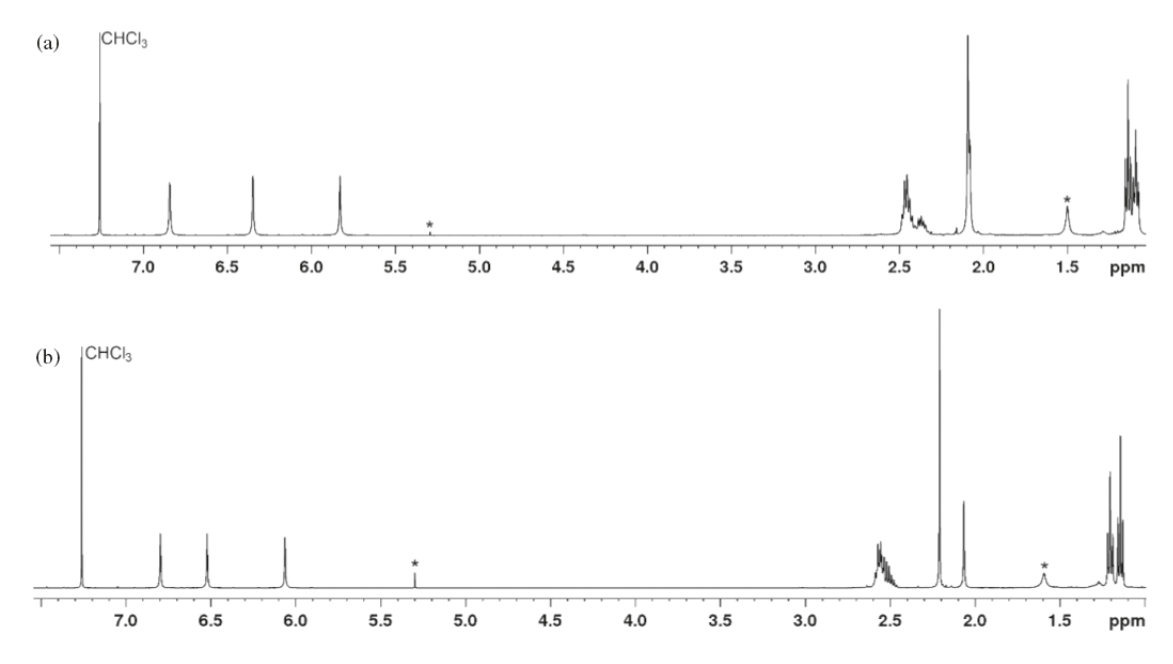


Fig. 6. 500 MHz proton NMR spectra of nickel(II) complex 19a (a) and palladium(II) complex 19c (b) in CDCl<sub>3</sub>.

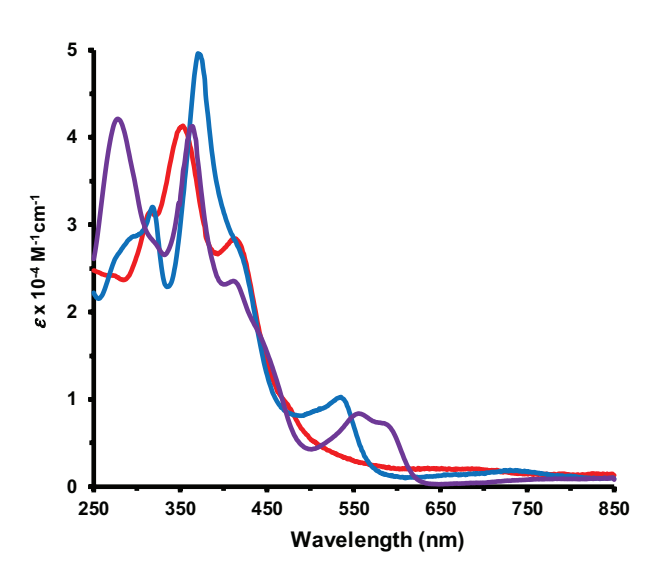
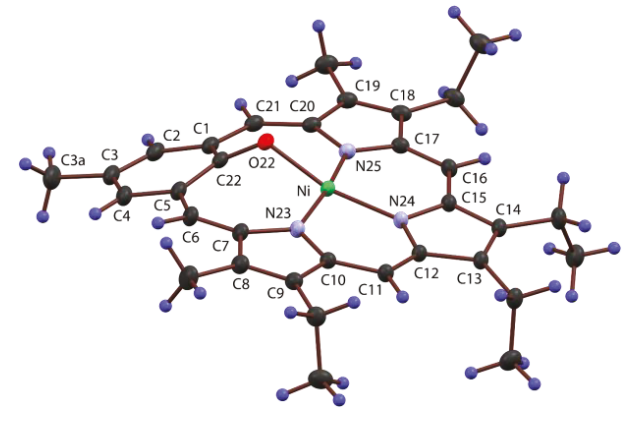


Fig. 7. UV-vis spectra of metal complexes 19a–19c in CH<sub>2</sub>Cl<sub>2</sub>. Red line: nickel complex 19a. Blue line: copper complex 19b. Purple line: palladium complex 19c.

**15** (M = Ni) has been synthesized previously, its X-ray structure was not obtained and this precluded direct bond metric comparisons [27].

The molecular structure for palladium complex **19c** (Fig. 9) adopts a conformation very similar to that observed for nickel complex **19a**, although the phenolate unit is pivoted further away from the macrocyclic plane. Relative to the mean plane defined by the tripyrrolic framework atoms, the pyrrole rings are tilted 1.7 (1)°, 6.24 (9)° and 4.94 (9)° However, the phenolic moiety is substantially canted by 40.89 (4)°, which is nearly 19°



**Fig. 8.** Color POV-Ray rendered Mercury-ORTEP III drawing (50% probability level, hydrogen atoms rendered arbitrarily small for clarity) of nickel complex **19a**.

more than observed for complex **19a**. A similar analysis relative to the three nitrogens ( $N_3$ ) gives dihedrals to the pyrrolic rings equal to 7.9 (1)°, 12.5 (1)° and 11.5 (1)°, with the *p*-cresole moiety substantially canted by 47.41 (5)°. This cant is significantly smaller than the observed 62.1° dihedral angle between the plane of the phenolate unit and that of the three nitrogen atoms ( $N_3$ ) in the closely related *meso*-tetraphenyl analogue **15** (M = Pd) [27]. The lesser tilt observed in **19c** can be attributed to the absence of steric interactions with *meso*-substituents. Bond distances and angles were generally validated using a Mogul geometry check [34]. The 1.9771 (10) Å Pd1-O22 bond length was both identified by Mogul as slightly shorter than average (2.002 (10) Å) for similar bonding environments and is 0.015 Å shorter than the

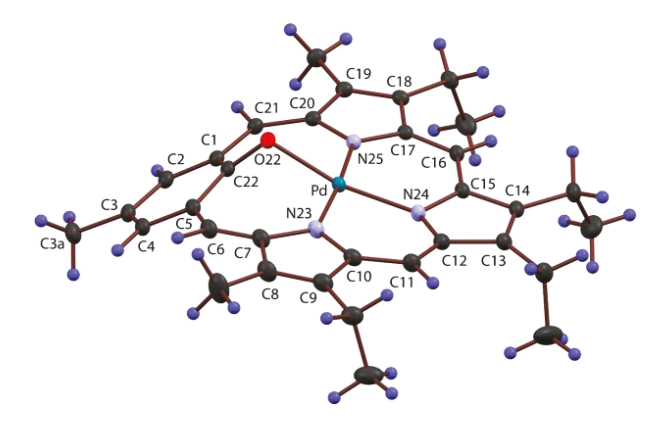


Fig. 9. Color POV-Ray rendered Mercury-ORTEP III drawing (50% probability level, hydrogen atoms rendered arbitrarily small for clarity) of palladium complex 19c.

1.992 (1) Å Pd-O separation observed for 15 (M = Pd). Complex **19c** exhibits a short 2.6703 (13) Å Pd1...C22 distance, which is significantly less than the sum of van der Waals radii (1.63 Å for Pd and 1.77 Å for C) [35], but is 0.10 Å longer than the 2.571 (2) Å Pd...C separation observed for 15 (M = Pd).

# CONCLUSIONS

Efficient syntheses of meso-unsubstituted 22-hydroxybenziporphyrins have been developed. Unlike the previously reported tetraphenyl-analogue, these benziporphyrins are reasonably stable, although the proton NMR spectra for the free bases were consistent with the presence of an antiaromatic species. The corresponding dications in TFA-CDCl3 gave well resolved proton and carbon-13 NMR spectra that confirmed the presence of a plane of symmetry. The dications showed only weakly diatropic characteristics and these species are essentially nonaromatic. Metalation of 22-hydroxybenziporphyrin 10a gave stable nickel(II), copper(II) and palladium(II) complexes. X-ray crystallography demonstrated that the nickel and palladium complexes were nonplanar with the phenolate ring pivoted away from the mean macrocyclic plane. Overall, the results demonstrate that mesounsubstituted hydroxybenziporphyrins have significantly different reactivity from their meso-tetraphenyl congeners, and the relative stability of these antiaromatic porphyrinoids makes them suitable for further investigation.

# Acknowledgments

This work was supported by the National Science Foundation under grant CHE-1855240. Further support from the National Science Foundation was obtained through the Major Research Instrumentation Program under grants CHE-1039689 (X-ray diffractometer) and CHE-0722385 (500 MHz NMR spectrometer). The authors also thank Dr. Steven Peters and Tony Ludwig for their assistance in running the low temperature NMR spectra.

# **Supporting information**

Crystallographic experimental details and selected <sup>1</sup>H NMR, <sup>1</sup>H–<sup>1</sup>H COSY, HSQC, DEPT-135, <sup>13</sup>C NMR, UV-vis spectra and mass spectra are provided. This material is available free of charge via the Internet at https://www.worldscientific.com/doi/suppl/10.1142/ S1088424621501030.

Crystallographic data have been deposited at the Cambridge Crystallographic Data Centre (CCDC) under numbers CCDC-2083958 and CCDC-2083959. Copies can be obtained on request, free of charge, via https:// www.ccdc.cam.ac.uk/structures/ or from the Cambridge Crystallographic Data Centre, 12 Union Road, Cambridge CB2 1EZ, UK (fax: +44 1223-336-033 or email: deposit@ ccdc.cam.ac.uk).

#### REFERENCES

- 1. Furuta H, Asano T and Ogawa T. J. Am. Chem. Soc. 1994: **116**: 767–768.
- 2. Chmielewski PJ, Latos-Grażyński L, Rachlewicz K and Glowiak T. Angew. Chem., Int. Ed. Engl. 1994; **33**: 779–781.
- 3. (a) Srinivasan A and Furuta H. Acc. Chem. Res. 2005; 38: 10-20. (b) Toganoh M and Furuta H in Handbook of Porphyrin Science — With Applications to Chemistry, Physics, Material Science, Engineering, Biology and Medicine, Vol. 2, Kadish KM, Smith KM and Guilard R. (Eds.), World Scientific Publishing: Singapore, 2010; Chapter 10, pp. 103-192.
- 4. Latos-Grażyński L in The Porphyrin Handbook; Kadish KM, Smith KM and Guilard R. (Eds.), Academic Press: San Diego, 2000; Vol. 2, pp. 361-416.
- 5. (a) Lash TD in Handbook of Porphyrin Science With Applications to Chemistry, Physics, Material Science, Engineering, Biology and Medicine, Vol. 16, Kadish KM, Smith KM and Guilard R. (Eds.), World Scientific Publishing: Singapore, 2012; Chapter 74, pp. 1-329. (b) Lash TD. Chem. Rev. 2017; 117: 2313-2446.
- 6. Lash TD. Org. Biomol. Chem. 2015; 13: 7846–7878.
- 7. (a) Lash TD and Hayes MJ. Angew. Chem., Int. Ed. Engl. 1997; **36**: 840–842. (b) Lash TD, Hayes MJ, Spence JD, Muckey MA, Ferrence GM and Szczepura LF. J. Org. Chem. 2002; 67: 4860-4874.
- 8. (a) Lash TD and Chaney ST. Angew. Chem., Int. Ed. Engl. 1997; 36: 839-840. (b) Lash TD. Acc. Chem. Res. 2016; 49: 471–482.
- 9. (a) Lash TD and Chaney ST. Tetrahedron Lett. 1996; 37: 8825-8828. (b) Bergman KM, Ferrence GM and Lash TD. J. Org. Chem. 2004; 69: 7888-7897.
- 10. Lash TD. Angew. Chem., Int. Ed. Engl. 1995; 34: 2533-2535.

- 11. Lash TD and Chaney ST. Chem. Eur. J. 1996; 2: 944-948.
- 12. Lash TD, Chaney ST and Richter DT. J. Org. Chem. 1998; **63**: 9076–9088.
- 13. AbuSalim DI and Lash TD. Org. Biomol. Chem. 2014; **12:** 8719–8736.
- 14. Lash TD, Rasmussen JM, Bergman KM and Colby DA. Org. Lett. 2004; 6: 549–552.
- 15. El-Beck JA and Lash TD. Org. Lett. 2006; 8: 5263-5266.
- 16. Stepien M, Latos-Grażyński L, Lash TD and Szterenberg L. Inorg. Chem. 2001; 40: 6892–6900.
- 17. Pokharel K, Ferrence GM and Lash TD. J. Porphyrins Phthalocyanines 2017; 21: 493-501.
- 18. Richter DT and Lash TD. Tetrahedron 2001; 57: 3659-3673.
- 19. Chaney, ST. MS Thesis, Illinois State University, 1997.
- 20. Johnson AL and Lash TD. 227th National Meeting of the American Chemical Society, Anaheim, CA, March 28-April 1, 2004. Book of Abstracts, CHED
- 21. Stepien M and Latos-Grażyński L. Chem. Eur. J. 2001; **7**: 5113–5117.
- 22. Stepien M and Latos-Grażyński L. Acc. Chem. Res. 2005; 38: 88-98.
- 23. Lash TD and Yant VR. Tetrahedron 2009; 65: 9527-9535.
- 24. Stepien M, Latos-Grażyński L, Szterenberg L, Panek J and Latajka Z. J. Am. Chem. Soc. 2004; **126**: 4566-4580.
- 25. (a) Lash TD, Young AM, Rasmussen JM and Ferrence GM. J. Org. Chem. 2011; 76: 5636–5651. (b) Lash TD, Toney AM, Castans KM and Ferrence GM. J. Org. Chem. 2013; 78: 9143-9152.

- 26. Lash TD, Szymanski JT and Ferrence GM. J. Org. Chem. 2007; 72: 6481-6492.
- 27. Stepien M and Latos-Grażyński L. Inorg. Chem. 2003; 42: 6183-6193.
- 28. Stepien M, Latos-Grażyński L and Szterenberg L J. Org. Chem. 2007; 72: 2259-2270.
- 29. (a) Lash TD. Chem. Eur. J. 1996; 2: 1197-1200. (b) Lash TD. J. Porphyrins Phthalocyanines 2016; **20**: 855–888.
- 30. (a) Sessler JL, Johnson MR and Lynch V. J. Org. Chem. 1987; 52: 4394-4397. (b) Lash TD. J. Porphyrins Phthalocyanines 1997; 1: 29-44.
- 31. Berlin K and Breitmaier E. Angew. Chem., Int. Ed. Engl. 1994; 33: 1246-1247.
- 32. (a) Colby DA, Ferrence GM and Lash TD. Angew. Chem. Int. Ed. 2004; 43: 1346-1349. (b) Lash TD, Colby DA, El-Beck JA, AbuSalim DI and Ferrence GM. Inorg. Chem. 2015; 54; 9174-9187. (c) Adiraju VAK, Ferrence GM and Lash TD. Org. Biomol. Chem. 2016; 14: 10523-10533.
- 33. (a) Xiao Z, Patrick BO and Dolphin D. *Inorg. Chem.* 2003; **42**: 8125–8127. (b) Rachlewicz K, Wang S-L, Ko J-L, Hung C-H and Latos-Grażyński L. J. Am. Chem. Soc. 2004; 126: 4420-4431. (c) Hung C-H, Wang S-L, Ko J-L, Peng C-H, Hu C-H and Lee M-T. Org. Lett. 2004; 6: 1393-1396.
- 34. Bruno IJ, Cole JC, Kessler M, Luo J, Motherwell WDS, Purkis LH, Smith BR, Taylor R, Cooper RI, Harris SE and Orpen AG. J. Chem. Inf. Comput. Sci. 2004; 44: 2133-2144.
- 35. Bondi A. J. Phys. Chem. 1964; 68: 441.